Chemistry–A European Journal
Review
doi.org/10.1002/chem.202404217
Chemistry Europe
European Chemical Societies Publishing

www.chemeurj.org

Advances in Chiral Macrocycles: Molecular Design and Applications

Zhihong Sun,[a] Hao Tang,*[a] Lingyun Wang,[a] and Derong Cao*[a]

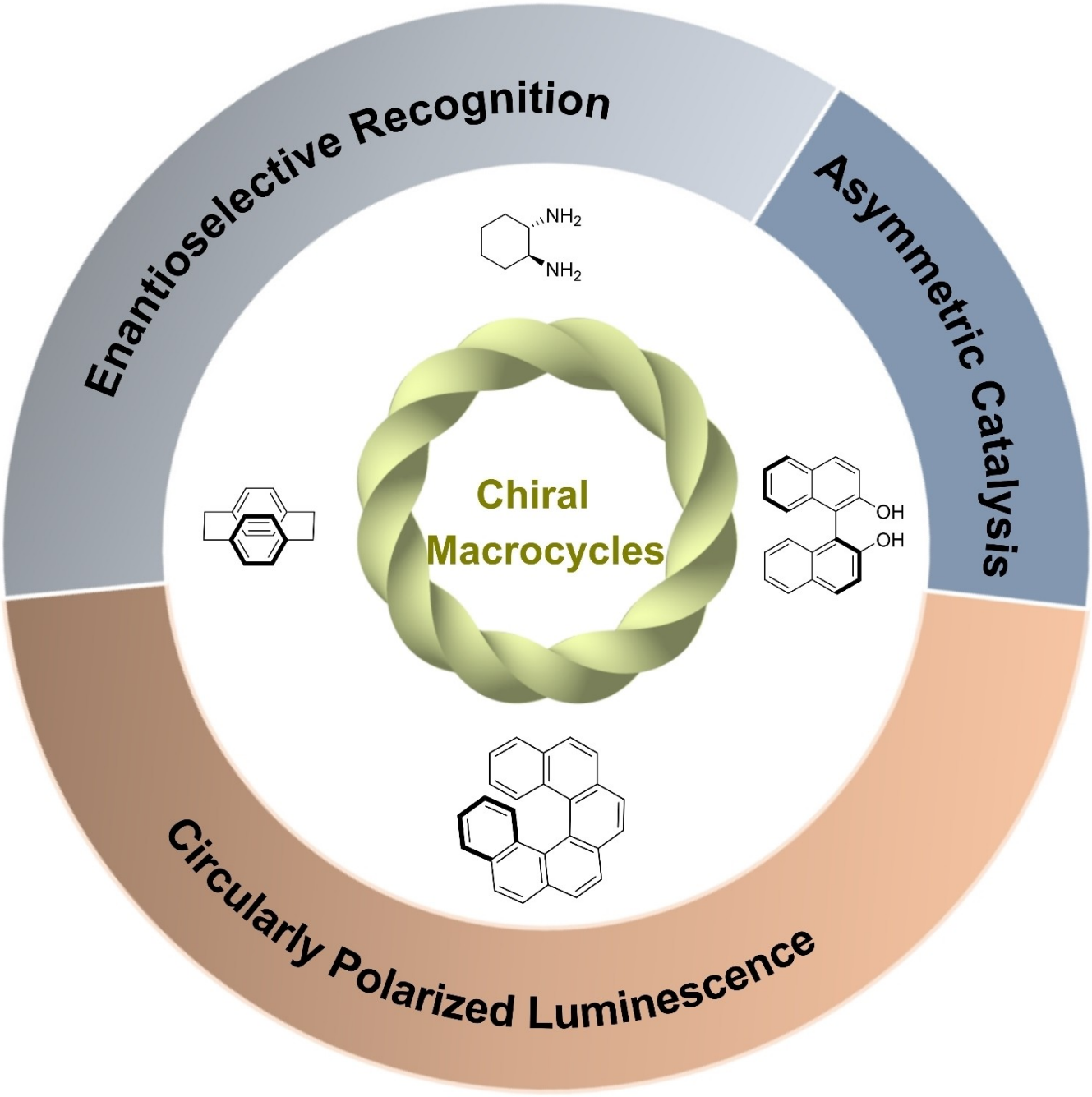

Chiral macrocycles have recently emerged as promising materials for enantioselective recognition, asymmetric catalysis, and circularly polarized luminescence (CPL) due to their terminal-free structure, preorganized chiral cavities, and unique host-guest and self-assembly properties. This review summarizes recent advances in the design and synthesis of chiral macrocycles with central, axial, helical, and planar chirality, each imparting distinct structural and chiroptical characteristics. We highlight key strategies for constructing these macrocycles and their applications in optoelectronic and catalytic systems. Emphasis is placed on the balance between rigidity and flexibility in macrocycle design, essential for effective molecular recognition, adaptable catalysis, and CPL. We conclude with perspectives on future opportunities, anticipating ongoing developments in chiral macrocycle research.

1. Introduction

Chirality is a fundamental symmetry property of matter at various hierarchical levels, present in both natural and synthetic materials.[1–4] An object is chiral if it cannot coincide with its mirror image.[5,6] Since the identification of chirality on the resolution of tartaric acids in 1848, molecular and supramolecular chirality has fascinated generations of chemists, leading to applications in chiral synthesis, molecular recognition, asymmetric catalysis, and circularly polarized luminescence (CPL, referring to the different emission between left- and right-circularly polarized light, which reflects the conformational information of chiral materials in the excited state.[7,8]).[9–14] Central chirality arises when a central carbon atom is bonded to four different substituents. Axial chirality results from the spatial arrangement of groups around an axis, while planar chirality originates from out-of-plane groups relative to a reference plane. Helical chirality involves the twisting of the backbone or substituents.[15]

Macrocycles, as receptor molecules with cavities, enable the arrangement of structural elements, the formation of binding sites, and the realization of specific functions.[16,17] Chiral macrocycles, formed by the introduction of chirality into macrocyclic structures, combine the advantages of both, offering a preorganized chiral microenvironment and unique host-guest interactions. Compared with acyclic molecules, the preorganized chiral cavity endowed cyclic analog with unique host-guest properties. Besides, macrocycles can impart severe restriction on bond rotations and component units flipping that can lock functional groups or other molecular fragments in conformations.[18,19] Various chiral macrocycles have been synthesized within systems such as crown ethers,[20,21] cyclodextrins,[22] cucurbiturils,[23] calixarenes[24] and pillararenes[25–27] and applied in enantioselective recognition, separation, catalysis and CPL.[28–32]

Chiral macrocycles serve as good candidates for chiral recognition owing to their well-defined cavities and multiple noncovalent interactions. Enantioselective recognition is of significance in understanding complex biological phenomena, developing chiral separation materials and constructing asymmetrically catalytic systems. The chiral recognition ability is determined by the noncovalent interactions between chiral hosts and different enantiomeric guests. For example, to improve enantioselectivity in aqueous system, it is important to design chiral macrocycles with a deep, well-defined hydrophobic cavity possessing polar binding sites.[33] Moreover, the precise control over cavity size, geometry and structures make chiral macrocycles promising candidates for asymmetric catalysis. Furthermore, CPL-active macrocycles have attracted increasing attention due to their symmetry, π-conjugated structures and self-assembly properties and their potential applications in encrypted information storage, organic light-emitting diodes, and 3D displays.[34–39]

Chiral macrocycles have generated significant interest over the past decade, with the scope of research gradually expanding from macrocycle synthesis and chiroptical properties to applications in chiral recognition, asymmetric catalysis, chiral supramolecular assembly, and CPL. This review primarily summarizes the developments in various types of chiral macrocycles over the last five years, focusing on the molecular design strategies that underpin their stereochemical properties and applications. The goal of this review is to highlight the exciting discoveries in this field and provide inspiration for the design of new chiral macrocycles and assemblies. For a broader review on topics such as CPL in chiral π-conjugated nanostructures, please refer to previously published literature.[40,41]

2. Molecular Design of Chiral Macrocycles

Chiral macrocycles can be classified based on their chiral elements into central, axial, planar, and helical chirality. Each type of chiral element imparts macrocycles unique structural and chiroptical properties, contributing to diverse applications. Methods for constructing chiral macrocycles include (i) introducing chiral substituents at the portals of achiral macrocycles, (ii) using chiral building blocks as skeletons, (iii) chiral guest induction, and (iv) symmetry breaking. Among them, using chiral building blocks as the skeleton to synthesize chiral macrocycles is the most popular method. Several typical building blocks for constructing chiral macrocycles are listed in Figure 1.

[a] Z. Sun, H. Tang, L. Wang, D. Cao
State Key Laboratory of Luminescent Materials and Devices, Department of Chemistry, School of Chemistry and Chemical Engineering, South China University of Technology, Guangzhou 510641, China
E-mail: htang@scut.edu.cn
drcao@scut.edu.cn

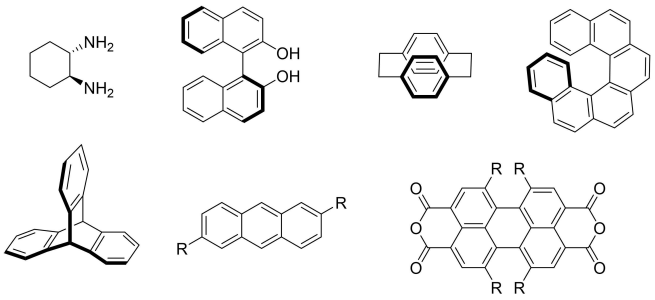

Figure 1. Representative building blocks for chiral macrocycles synthesis.

2.1. Macrocycles Containing Central Chirality

The introduction of central chirality is one of the simplest ways to construct chiral macrocycles. While central chirality can be introduced post-synthetically with chiral carbon substituents, the most widely used strategy for creating configurationally stable macrocycles with central chirality is through the use of chiral bridge units, e.g., chiral imine or imide.[42] The selection of bridge units not only influences the shape and conformation of chiral macrocycles but also affects chirality transfer and the properties of the resulting assemblies. Among those, *trans*-1,2-diaminecyclohexane, with its C_2 symmetry and rigid cyclohexane skeleton, is often chosen as a building block for synthesizing chiral macrocycles.[43] Stoddart et al.[44] developed a strategy to synthesize a series of molecular triangles via condensation reactions, using *trans*-1,2-diaminecyclohexane and aromatic tetracarboxylic diimide (ADI) as the apexes and linkers, respectively (Figure 2a). The molecular chirality originates from *trans*-1,2-diaminecyclohexane, whereas ADI building blocks including pyromellitic diimide (PMDI), naphthalene diimide (NDI) and perylene diimide (PDI) define the overall geometry, functionalities, and assembly potential.[44–47] With a spatially restricted chiral microenvironment, these molecular triangles act as promising candidates for enantioselective recognition, asymmetric catalysis and chiral assembly. By introducing various groups into the π-conjugated linkers, the electronic, optical and magnetic properties of these triangles can be tuned, resulting in a range of functional chiral materials. Given their electron-deficient units, Stoddart and coworkers[45] used NDI-based triangles as electron acceptors, and 9,10-dichloroanthracene (DCA) and 1-chloronaphthalene (CN) as electron donors, preparing two cocrystals (Figure 2b). Remarkably, these cocrystals demonstrated reversible cocrystal-to-cocrystal transformations upon exchanging electron donors. Inspired by the above synthesis strategy, Liu and coworkers[42] synthesized a chiral triangle **T1** (Figure 2c) employing the *trans*-1,2-diaminecyclohexane and dialdehyde-functionalized pyrenes as vertices and edges, respectively. The *trans*-1,2-diaminecyclohexane ensured configurational chirality in **T1**, while the zigzag-shaped pyrene building block conferred conformationally dynamic planar chirality. At the molecular state, chirality only originates from point chirality of the vertices; however, upon self-assembly, planar chirality emerged due to restricted rotation of the pyrene edges, ultimately prevailing over point chirality. These studies underscore the importance of selecting proper linkers, as they not only define the shape and optical properties of the macrocycles, but also significantly influence chirality transmission during the assembly process.

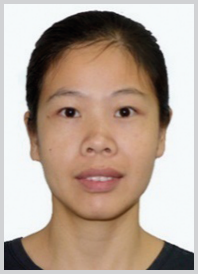

Zhihong Sun received her B.E. in 2012 from Hebei University of Technology and her master's degree in 2015 from Tianjin University. She is currently a Ph.D. candidate at South China University of Technology under the supervision of Prof. Derong Cao. Her research interest focuses on functional chiral macrocycles synthesis and their supramolecular assemblies.

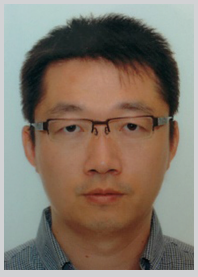

Prof. Hao Tang received his B.S. and M.S. degrees from Wuhan University and completed his Ph.D. under the guidance of Prof. Cornelia Bohne at the University of Victoria, Canada, in 2011. Following this, he conducted postdoctoral research with Prof. Elena Galoppini at Rutgers University. In 2016, he joined South China University of Technology as a professor. His research focuses on elucidating the molecular recognition mechanisms of various supramolecular systems, particularly through kinetic studies, and investigating how macrocycle structures impact their performance in artificial light-harvesting systems, adsorption-based separation, probes, and other applications.

Prof. Lingyun Wang earned her Ph.D. in Chemistry from Sun Yat-Sen University, China, in 2006. Following postdoctoral training at South China University of Technology (SCUT), she joined SCUT, where she is now a professor in the School of Chemistry and Chemical Engineering. Her research currently centers on the design and synthesis of functional NIR fluorescent dyes and their applications in chemosensors, biosensors, and optoelectronics.

Prof. Derong Cao studied Chemistry at Lanzhou University, China, and completed his doctoral thesis in Organic Chemistry in 1997 under the supervision of Prof. Herbert Meier at the University of Mainz, Germany, and Prof. Li at Lanzhou University. He became an Associate Professor at Lanzhou University in 1997 and was promoted to Full Professor at the Guangzhou Institute of Chemistry, Chinese Academy of Sciences, in 2002. Currently, he is affiliated with the School of Chemistry and Chemical Engineering at South China University of Technology, Guangzhou. His primary research interests lie in organic functional molecules and materials.

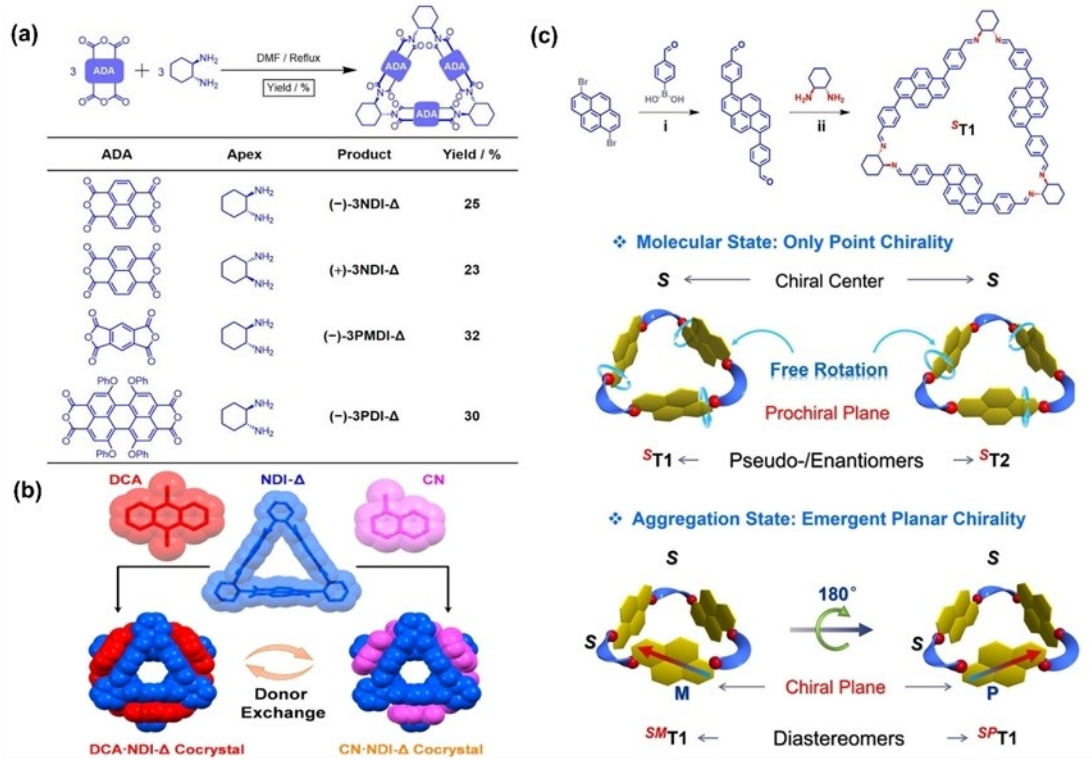

Figure 2. (a) Synthesis of molecular equilateral triangles; (Reproduced from Ref.[44] with permission. Copyright 2021 American Chemical Society.) (b) Cocrystal-to-cocrystal; (Reproduced from Ref.[45] with permission. Copyright 2023 American Chemical Society.) (c) Synthesis of triangle **T1**. (Reproduced from Ref.[42] with permission. Copyright 2022 Wiley-VCH GmbH.)

2.2. Macrocycles Containing Axial Chirality

Axially chiral compounds exhibit chirality through the spatial arrangement around a rotational axis. Axially chiral macrocycles primarily inherit chirality from their axially chiral building blocks, including substituted allenes, alkylidenecycloalkanes, biaryls, spiranes, binaphthol, and adamantoid structures. Among these building blocks, the binaphthol (BINOL) skeleton is one of the most representative axial building blocks, known for its stable chiral configuration, ease of modification, and commercial availability.[48,49] Reported chiral macrocycles can be categorized into conjugated and non-conjugated types.

Conjugated macrocycles are shape-persistent, exhibit certain rigidity, and display strong fluorescence, which makes them good candidates for CPL and chiral recognition. Due to the large size of BINOL, the synthesized macrocycles inherently possess deep aromatic cavities, making them well-suited for molecular recognition. Cyclic π-conjugated structures can be synthesized through homo-coupling reaction[50] or cross-coupling reaction such as Suzuki and Sonogashira reaction.[51,52] Recently, Cai group designed and synthesized a pair of enantiomeric water-soluble fluorescent macrocycles, *RRRR*-**C[4]BINOL** and *SSSS*-**C[4]BINOL**.[53] The enantiomerically pure products was synthesized via a $Ni(cod)_2$-mediated Yamamoto homo-coupling reaction, followed by a hydrolysis reaction (Figure 3a). Single crystal X-ray analysis showed that *RRRR*-**C[4]BINOL** adopts a tubular conformation with a cavity depth around 10.0 Å, which is comparable to that of cucurbit[n]urils. **C[4]BINOL** with electron-rich and deep hydrophobic cavity demonstrated excellent enantioselectivity (up to 18.7) towards chiral **SPINOL** (Figure 3b) in aqueous solution. Moreover, **C-[4]BINOL** also exhibited remark high recognition affinities (up to $10^{12}\ M^{-1}$) towards 16 important steroidal compounds (Figure 3c) as well as good enantioselectivity (up to 15.5) in water.[54] Similarly, Cai and coworkers also constructed other deep conjugated macrocycles with biphenyl building blocks via Suzuki cross-coupling reaction.[55] These results illustrated that constructing deep aromatic cavities with lengthy axial building blocks in aqueous systems can greatly enhance the hosting ability and enantioselective recognition properties.

Non-conjugated macrocycles exhibit greater flexibility compared to conjugated ones, and the balance between rigidity and flexibility is particularly important for specific receptor-substrate interactions.[16] Li et al.[56] incorporated the BINOL skeleton into biphenarenes synthesis, and prepared a pair of chiral macrocycles (*R*/*S*)-**BINOL[2])** (Figure 4a) in two synthetic steps with yields over 60%. (*R*/*S*)-**BINOL[2]** with inward-directing OH groups display an enantioselectivity value of 13.2 towards chiral ammonium salts (Figure 4b), which is attributed to noncovalent interactions and desirable cavities. This study illustrates that various chiral macrocycles with desirable properties can be designed and constructed by combing the axial chiral units with other macrocyclic arenes synthesis building blocks.

Axially chiral macrocycles, designed with cavities and noncovalent interactions, are valuable for various types of asym-

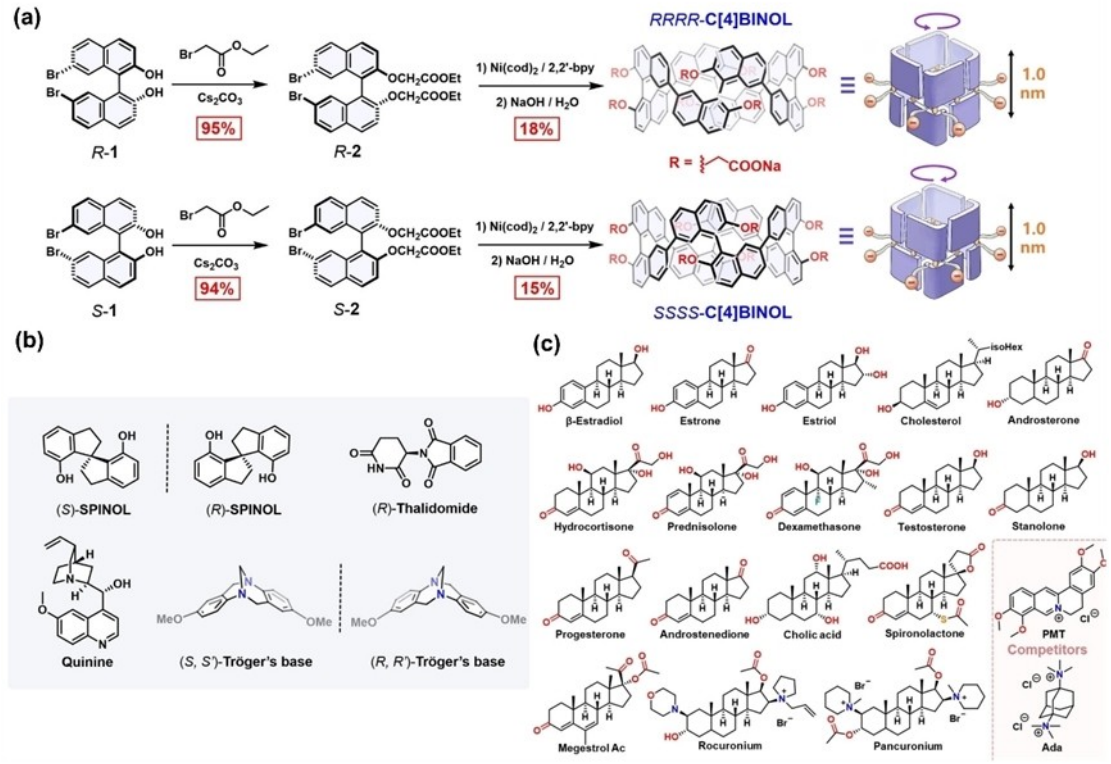

Figure 3. (a) Synthetic routes of *RRRR*-**C[4]BINOL** and *SSSS*-**C[4]BINOL**; (b) Chemical structure of chiral guests; (Reproduced from Ref.[53] with permission. Copyright 2023 Wiley-VCH GmbH.) (c) Chemical structure of chiral steroidal. (Reproduced from Ref.[54] with permission. Copyright 2024 Wiley-VCH GmbH.)

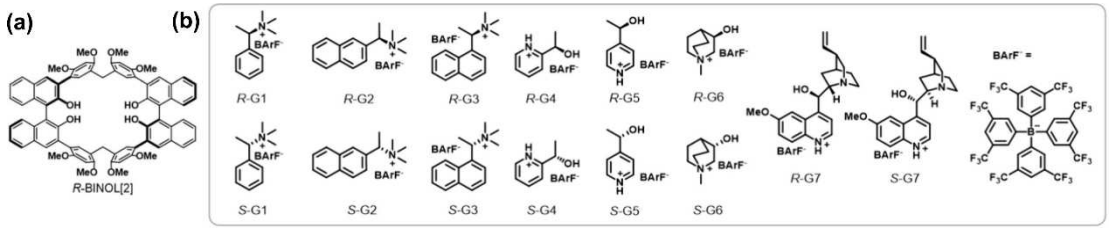

Figure 4. (a) Chemical structure of R-**BINOL[2]**; (b) Chemical structure of guests. (Reproduced from Ref.[56] with permission. Copyright 2024 American Chemical Society.

metric catalysis. Inspired by natural enzyme catalysis, chiral macrocycles with carefully engineered host-guest properties have been synthesized to enhance their application in asymmetric catalytic processes.[57] Enantiomeric excess (ee) is the percentage difference between the mole fractions of the two enantiomers, quantifying the enantiomeric composition and indicating the enantioselectivity of asymmetric catalysis. Higher ee reflects greater catalytic selectivity. Ishihara et al.[58] designed a macrocyclic lithium binaphtholate catalyst for the enantioselective addition of lithium acetylide to different ketones (Figure 5), achieving high reactivity and selectivity attributed to the cavity effect and the lipophilic effect. The macrocyclic cavity effectively prevents undesired aggregative deactivation, while the lipophilicity of macrocycle imparts substrates specificity. Wang and coworkers offer another strategy using well-defined catalytic groups as building blocks to construct macrocycles. They designed chiral macrocycles with two phosphate sites in

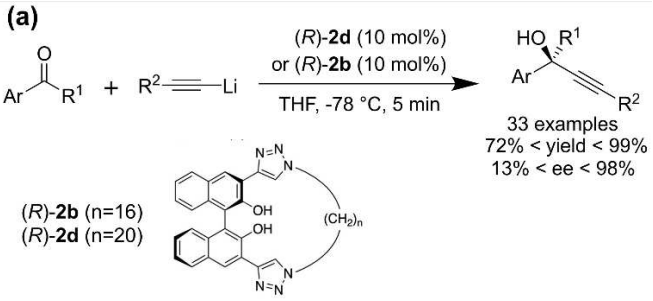

Figure 5. (a) Enantioselective addition of lithium acetylides to ketones.

tunable distance, which form a strong ion-pair interaction with dicationic selectfluor.[59] In catalytic enantioselective fluorination (Figure 6), only 2 mol% of the macrocyclic catalyst yielded the desired products in moderate yields and up to 91% ee. The

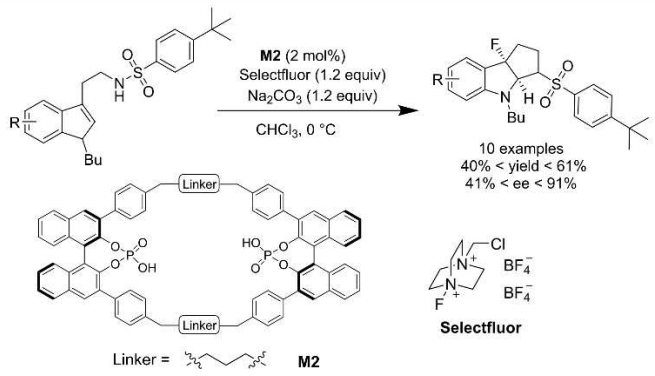

Figure 6. Enantioselective Fluorcyclization.

high catalytic performance is attributed to the tight ion-pair binding and cavity-directed multiple noncovalent interactions. Furthermore, by applying a macrocycle-enabled counteranion trapping strategy, the Wang group[57] developed an axially chiral macrocycle containing diarylthiourea binding sites This macrocycle, combined with ethanedisulfonic acid, promoted excellent conversion and stereocontrol in the Friedel–Crafts reaction of indoles with imines (Figure 7), demonstrated the potential of axially chiral macrocycles in asymmetric catalysis.

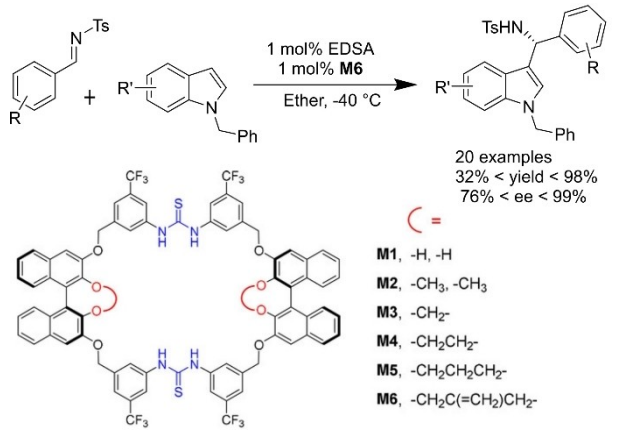

Figure 7. Friedel-Craft reaction of indoles with aldimines.

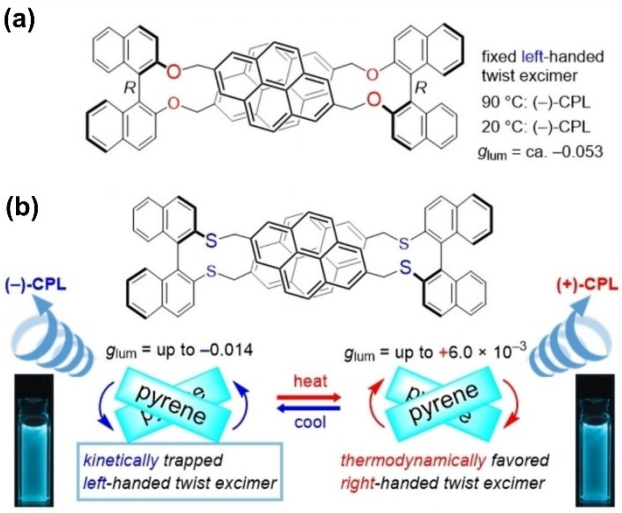

Figure 8. (a) Chemical structure of (*R*,*R*)-**2**; (b) Chemical structure of thioether-linked pyrenophanes. (Reproduced from Ref. [61] with permission. Copyright 2024 Wiley-VCH GmbH.)

By adjusting the linkers in non-conjugated chiral macrocycles, it is possible to effectively control chirality inversion and signal intensity. The flexible linkers endow these macrocycles with more complex conformations, presenting intriguing potential applications in CPL. Ema and coworkers[60] first designed a series of D_2-symmetric macrocycles (*R*,*R*)-**2** (Figure 8a) consisting of pyrenes and binaphthyls, which was connected with different linkers. Binaphthyl-bridged pyrenophane (*R*,*R*)-**2** possessing ether linkers exhibits a luminescence dissymmetry factor (g_{lum}) value of −0.053. The expectational CPL performance is ascribed to the parallel transition dipole moments based on D_2 symmetry. When replacing the ether linker with thioether linker (Figure 8b), the macrocycles exhibited a temperature-induced sign inversion of CPL.[61] The pyrenes form left-handed twist excimer at low temperature but right-handed twist at high temperature. Instead of tuning the linker type, Meng et al.[62] simply synthesized three pair of BINOL based tetraphenylethylenes (TPEs) macrocycles with different linkage length, and the chiral macrocycle with the longest linkage exhibits a g_{lum} value of 1.9×10^{-3}.

The combination of CPL and aggregation-induced emission (AIE) enhances the CPL response in the aggregated state.[63–65] Stoddart group[66] designed and synthesized binaphthyl-based tetracationic cyclophanes, (*RR*)- and (*SS*)-6,6′ **BinBox**·4PF6, by inserting binaphthyl building block between two pyridinium units. Single crystal X-ray analysis shows a figure-eight geometry, which leads to an additional helicity (Figure 9a). The packing of macrocycles exhibits (Figures 9b) a tubular superstructure consisting of charge transfer (CT) interactions. Remarkably, these macrocycles exhibit efficient CPL performances both in solution and in the aggregated states (Figure 9c and d), and the typical AIE effect originates from limited torsional motions associated with the axial binaphthyl moieties.

2.3. Macrocycles Containing Helical Chirality

Helicenes are inherently chiral molecules, making their incorporation into macrocycle synthesis highly appealing due to their unique topology and potential for diverse applications. However, this approach faces significant synthetic challenges. Recently, several interesting conjugated hydrocarbon nanostructures have been reported. Moore et al.[67] synthesized a conjugated Möbius macrocycle from 2,13-bis(propynyl)[5]helicene via alkyne metathesis in 84 % yield. The direct cyclization is quite simple but afford heterochiral *PPM* and *MMP* macrocycles. Durola group[68] designed and synthesized a triply [5]helicene-bridged (1,3,5)cyclophane **G**, which is homochiral. To synthesize the constrained structure, they developed a glyoxylic Perkin strategy (Figure 10a) and applied in [5]helicene-containing rigid macrocycles. The resolution of

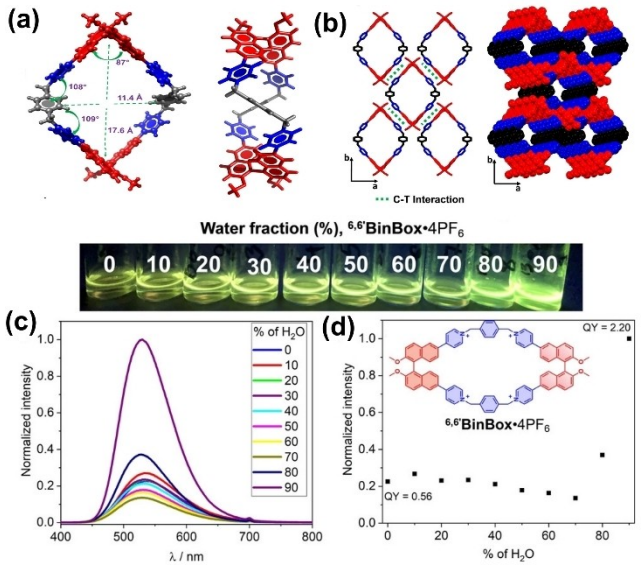

Figure 9. (a) X-ray crystal structure of (SS)-6,6′ **BinBox**·4PF6; (b) CT interactions and a tubular superstructure of macrocycle; (c) Normalized intensity of the emission spectra of (RR) /(SS)-6,6′ **BinBox**·4PF6; (d) Normalized intensity of QY of (RR) /(SS)-6,6′ **BinBox**·4PF6 in different solvent mixtures versus the percentage of H_2O. (Reproduced from Ref.[66] with permission. Copyright 2022 Wiley-VCH GmbH.)

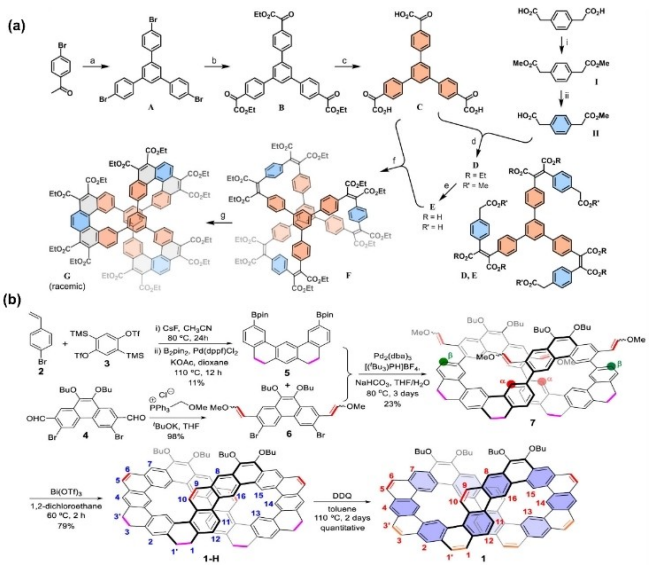

Figure 10. (a) Synthesis of the tris[5]helicenylene-cyclophane **G**; (Reproduced from Ref. [68] with permission. Copyright 2023 Wiley-VCH GmbH.) (b) Synthesis of the figure-eight macrocycles **1-H** and **1**. (Reproduced from Ref. [69] with permission. Copyright 2021 American Chemical Society.)

the enantiomers of **G** was achieved by high performance liquid chromatography (HPLC) and the enantiopure samples of (*P,P,P*)-**G** and (*P,P,P*)-**G** can finally be obtained. Similarly, Wu and coworkers[69] reported the synthesis and chiral resolution of chiral macrocycles with a figure-eight configuration. Macrocycles **1-H** was synthesized via Suzuki coupling reaction followed by Bi(OTf)3-catalyzed cyclization reaction, and the oxidative dehydrogenation of **1-H** afforded conjugated macrocycle **1** (Figure 10b).

The combination of helicene and other π-conjugated building blocks results in different topologic structures. Combining helicenes with conjugated units simplifies the synthesis of chiral macrocycles, while still enabling the construction of various topological structures. The figure-eight helical conformation demonstrates superior CPL performance. Šolomek group[70] integrated a [6]helicene into [7]cycloparaphenylene and synthesized a Möbius helicene carbon nanohoop. The target macrocycle was synthesized by Suzuki-Miyaura coupling reaction, followed by deprotection of protecting groups and reductive aromatization reaction. The chirality transfer from the [6]helicene induces a strong CPL in macrocycle, with a g_{lum} value of 2.2×10^{-3}. Chen[71] incorporated [5]helicene into triarylborane/ amine moieties and synthesized several chiral macrocycles (**CMC1**, **CMC2**, and **CMC3**) (Figure 11a). **CMC1** and **CMC2** adopting a figure-eight shape show a higher g_{lum} compared with **CMC3** with a diamond shape. By tuning the electron-withdrawing moieties, the emission spectra can red-shift from blue to near-infrared (NIR) region. Recently, Sabapathi group[72] synthesized (Figure 11b) a conformationally locked cyclo[2]Dipyrrins linked with achiral anthracene subunits. Single crystal X-ray analysis confirms the figure-eight helical conformations (Figure 11c), which is stabilized by intramolecular hydrogen bonding. The macrocycle exhibits CPL (Figure 11d) with a g_{lum} value around 3.8×10^{-3}.

2.4. Macrocycles Containing Planar Chirality

A macrocycle with a chiral plane exhibits planar chirality, where the cyclic skeleton restricts bond rotations of the aromatic ring,

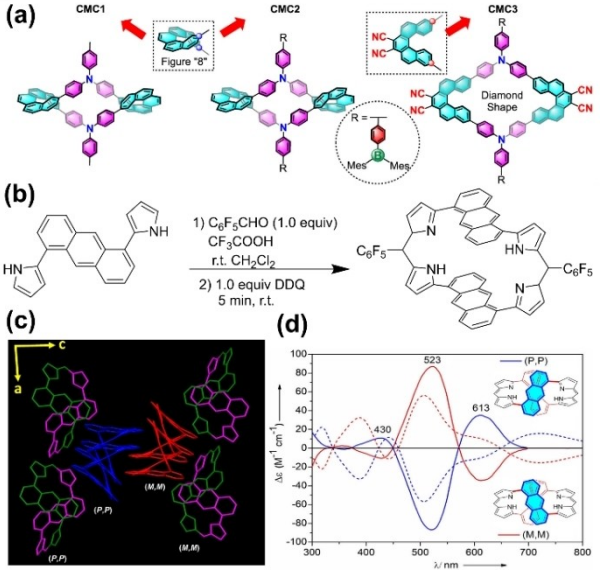

Figure 11. (a) Chemical Structure of **CMC1**, **CMC2**, and **CMC3**; (Reproduced from Ref.[71] with permission. Copyright 2023 American Chemical Society.) (b) Synthesis of Conformationally Locked Cyclo[2]Dipyrrins **1**; (c) X-ray structure of Cyclo[2]Dipyrrins **1**; (d) Experimental and simulated circular dichroism (CD) spectra for (P,P)-**1** (blue, first fraction) and (M,M)-**1** (red, second fraction) in THF. (Reproduced from Ref.[72] with permission. Copyright 2023 Wiley-VCH GmbH.)

locking three-dimensional chiral conformations.[19] The concept of planar chirality as a stereogenic unit was first introduced in 1956.[73] Since then, interest in strained macrocycles with planar chirality has grown, primarily focusing on cyclophanes.[74] Calixarene[75] is a cyclic oligomer based on a hydroxyl alkylation product of phenols and aldehydes, and the stereochemistry of the calixarenes have attracted attention since the beginning. There are numerous examples of chiral calixarenes and analogs, and readers can refer to related reviews[76–78] and recent published work.[79–81] Pillararenes, which were first introduced by Ogoshi's group[82] in 2008, are cylindrical macrocyclic hosts with intrinsic planar chirality.[83] Chiral pillararenes have been extensively investigated since its discovery, and more detailed information about the planar chirality in pillar[5]arenes, the reader is referred to some excellent reviews just published.[27,84–87]

Planar chirality is stereo-dynamic, so guest complexation[25,88] and the introduction of bulky substituents[89–90] are often used to restrict the rotation of benzene rings.[85] These strategies can extend to other macrocyclic arenes with planar chirality. For example, Chen et al.[91] selected 2,7-dimethoxynaphthalene as a building block to synthesize saucer[4]arene (H1) and saucer[5]arene (H2). The introduction of chiral quaternary ammonium guests induced the chirality of saucer[n]arenes, thus making the macrocyclic arenes exhibit CPL properties in the host–guest systems (Figure 12a). Similarly, Jiang group[92] designed a class of methylene-bridged naphthotubes, which was composed of alkoxy substituted bisnaphthalene clefts and synthesized by Friedel–Crafts reactions (Figure 12b). These naphthotubes are dynamic chiral (Figure 12c) and their planar chirality can be induced by chiral organic cations. In order to mimic bioreceptors, Jiang et al.[93] employed the concept of endo-functionalized cavity and synthesized a chiral amide naphthotubes (**1**, Figure 13a), which showed enantioselectivities up to 2.0 to *p*-benzoquinone. Moreover, based on these investigations, Jiang and coworkers[94] further improved their biomimetic design (Figure 13b) and introduced chiral centers close to the amide group to control the chirality and synthesized two pairs of enantiopure naphthotubes (**2** and **3**, Figure 13c). These naphthotubes exhibit highly enantioselective recognition toward 90 chiral guests in aqueous solution, achieving the highest enantioselectivity of 34 with neotame.

The combinations of host–guest complexation and aggregation provide an effective way to construct chiral functional materials.[95,96] Yang et al.[97] achieved a significant chiroptical response in pyrene-modified γ-CDs aggregates via a combination of host-guest interactions and supramolecular aggregations (Figure 14). Similarly, Chen and coworkers[98] adopted the host-guest interaction and constructed supramolecular polymer gels based on enantiomeric macrocycles and achiral guests, which exhibited an induced CPL and an enhanced emission. Cao et al.[99] synthesized an achiral anthracene-based tetracationic, which not only exhibited supramolecular chirality by host-guest complexation with nucleoside triphosphates, but also showed chirality by twisted packing.

Symmetry breaking is another effective way to construct chiral macrocycles. Jiang group[100] reported a series of chiral carbon nanohoops **TP-[8–13]** (Figure 15a) by embedding triptycene into [n]CPPs via symmetry breaking. The emission intensity and g_{lum} value of **TP-[n]CPPs** are size-dependent. **TP-[13]CPP** has the highest fluorescence quantum value of 92.9%, while **TP-[8]CPP** exhibits the highest g_{lum} value of 3.8×10^{-3}. Similarly, anthracene is a versatile building block to build novel chiral conjugated macrocycles.[101,102] Du et al.[103] reported **[*n*]CPPAn$_{2,6}$** (n = 6–8) macrocycles by incorporating anthracene into the C-shaped molecular scaffolds, and these macrocycles showed similar size-dependent trends in optical and chiroptical properties (Figure 15b).

The introduction of inherently chiral building blocks with preorganized geometry into macrocycle synthesis offers another way to construct macrocycle with static chirality. Wu et al.[104] used V-shaped Tröger's base as a building block to synthesize triangular macrocycles (Figure 16a). Although these macrocycles are heterochiral, they exhibit persistent chirality and chirality-dependent packing behavior. Similarly, Chen et al.[105]

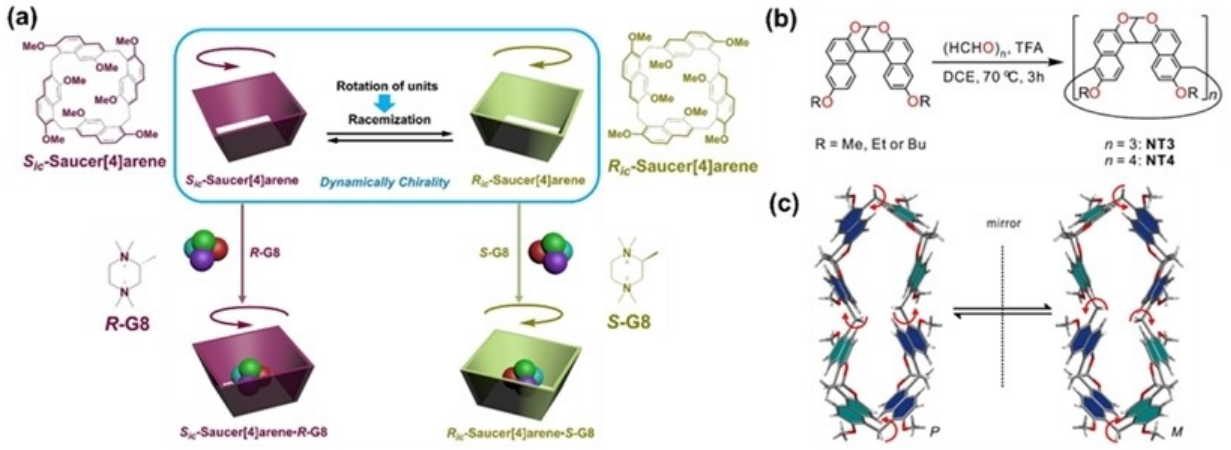

Figure 12. (a) Cartoon representation of competitive conformation chirality of saucer[n]arenes induced by chiral guests; (Reproduced from Ref.[91] with permission. Copyright 2023 Wiley-VCH GmbH.) (b) Synthetic procedures of methylene-bridged naphthotubes; (c) X-ray single crystal structure of NT4-Me which shows the two enantiomers. (Reproduced from Ref.[92] with permission. Copyright 2022 Wiley-VCH GmbH.)

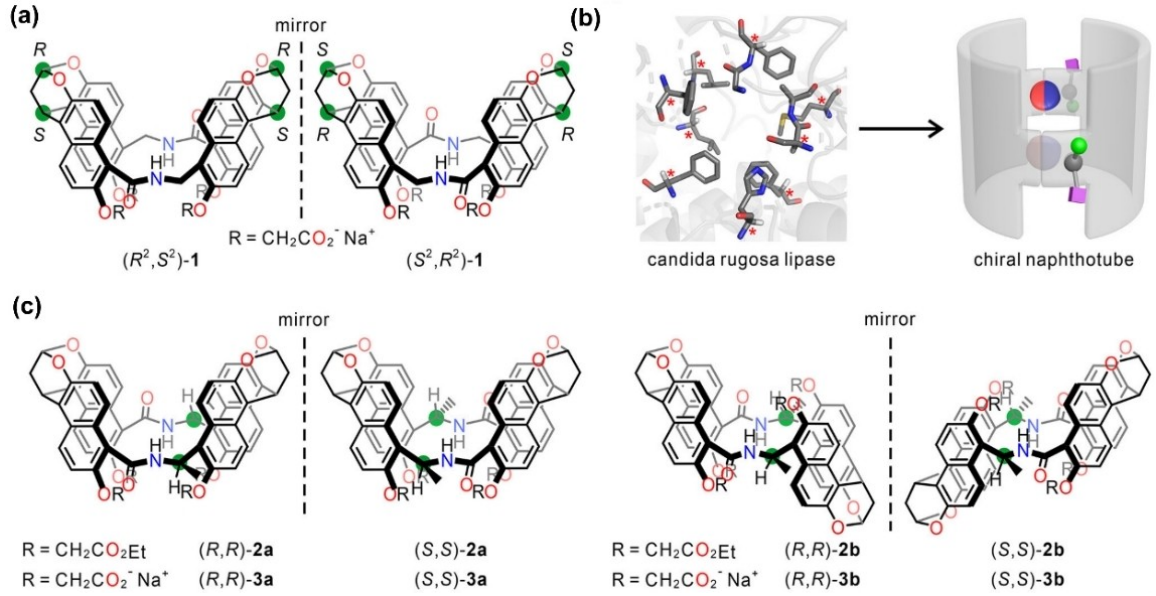

Figure 13. (a) Chemical structures of chiral naphthotubes **1**; (b) Biomimetic design of an endo-functionalized cavity with chiral centers located at the neighborhood of the inward-directing functional groups for chiral recognition in water; (c) Chemical structures of chiral naphthotubes **2** and **3**. (Reproduced from Ref.[94] with permission. Copyright 2024 American Chemical Society.)

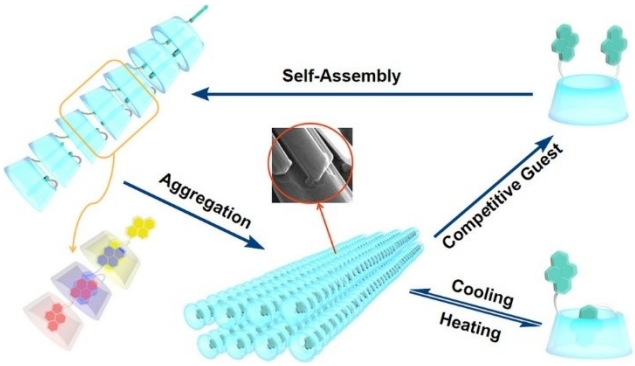

Figure 14. Schematic diagram of the aggregation processes of di-pyrene-substituted γ-CDs. (Reproduced from the Ref.[97] with permission. Copyright 2022 Wiley-VCH GmbH.)

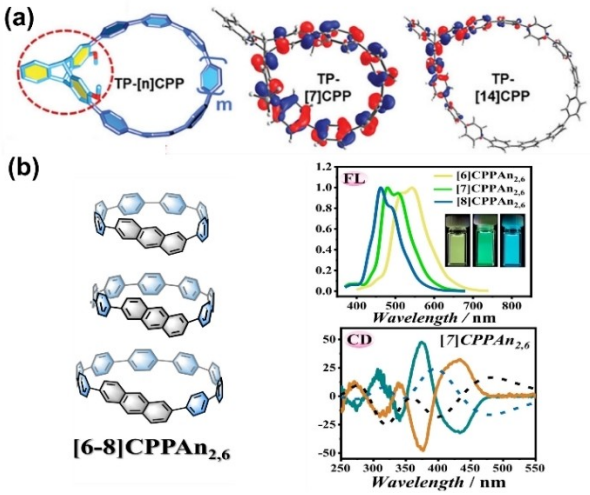

Figure 15. (a) Chiral conjugated nanohoops (TP-[n]CPPs) with breaking symmetry; (Reproduced from Ref.[100] with permission. Copyright 2023 Wiley-VCH GmbH.) (b) Chemical structures of [n]CPPAn2,6 and their optical and chiroptical properties. (Reproduced from Ref.[103] with permission. Copyright 2022 Wiley-VCH GmbH.)

synthesized a class of homochiral macrocycles **octopus[3]arenes** (Figure 16b), which are composed of ethenoanthracene subunits. The water-soluble macrocycles exhibit enantioselective recognition toward ammonium salts in aqueous solution with the association constant up to 10^6 and the enantioselectivity value up to 12.89. Zhu et al.[106] selected an achiral flipping panel (thianthrene) as a building block to afford a pair of homochiral macrocycles (Figure 16c). The introduction of phenylethynyl groups on the rim makes the macrocycles *P*-**7** and *M*-**7** exhibit CPL with a $|g_{lum}|$ value of 5×10^{-3}.

Perylene bisimides (PBIs), also called perylene diimides (PDIs), as an important class of organic dyes, have received increasing attention for applications in organic optoelectronics due to their favorable optical and redox properties.[107–110] They also exhibit conformational chirality because of the distortion of the π-system, which results from the repulsive interactions between the sterically bay substituents.[111,112] Cyclophanes derived from PBIs should be of particular interest. Würthner and coworkers[113] designed a chiral cyclophane composed of two core-twisted PBI units, which demonstrates strong noncovalent binding of non-planar aromatic guest molecules due to inherently conformational flexibility. More importantly, the chiral macrocycle exhibited a preferential binding of [5]helicene of opposite helicity, leading to heterochiral host-guest complex (Figure 17a), which could be further confirmed by a single crystal heterochiral complexes (Figure 17b). Based on previous research on host-guest properties of PBI-based macrocycles,[114,115] Würthner presented a highly twist PBI

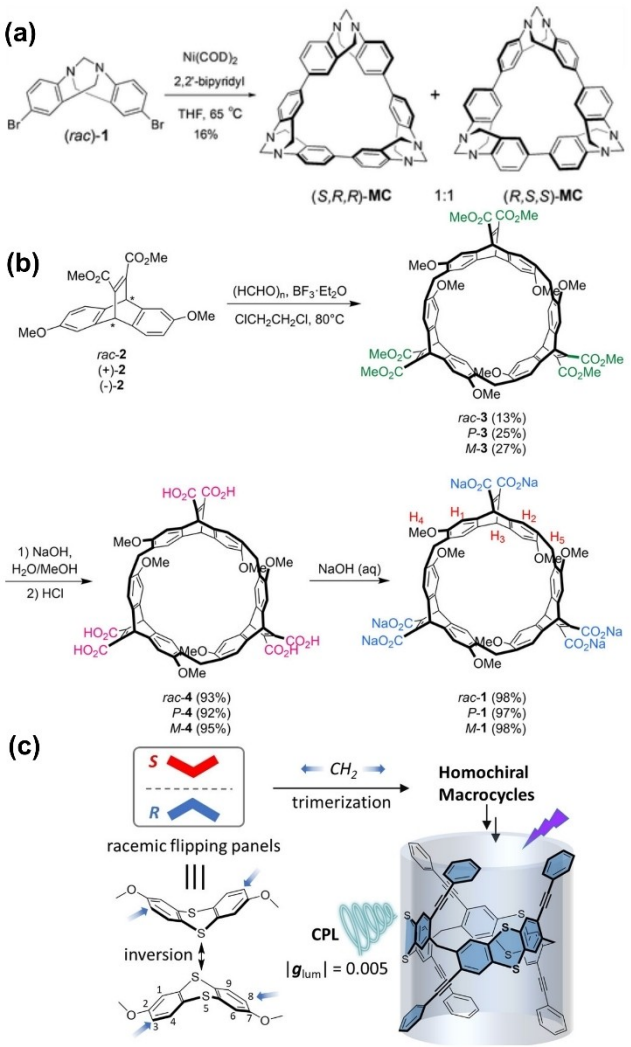

Figure 16. (a) Synthesis of Tröger's-base triangular macrocycles; (b) Synthesis of **octopus[3]arenes**; (c) Macrocyclization of a flipping monomer. (Reproduced from Ref.[106] with permission. Copyright 2023 Wiley-VCH GmbH.)

cyclophane,[116] with 1,7-bridging units connecting the two bay positions of the PBI moiety, then the PBI cyclophane was used as supramolecular catalysis to catalyze the enantiomerization (Figure 17c). The reaction kinetics was accelerated by a factor of ~700 at 295 K, which is ascribed to transition state stabilization from dispersion and electrostatic interactions. Through molecular design, a class of conformationally stable PDI macrocycles has been constructed, exhibiting unique assembly properties and chiral amplification capabilities. The preorganization of aromatic groups within these macrocycles promotes $\pi-\pi$ stacking interactions, thereby fine-tuning the macrocycle properties. Barendt group[117] developed a novel bis-PDI pink box, which exhibits a quite high value of CPL dissymmetry factor (10^{-2}) because of homochiral H-type aggregation. To further understand the connection between PDI chirality and H-/J-type aggregation, Barendt and coworkers[118] reported the first chirally locked bis-PDI macrocycle (Figure 18a) by introducing *tert*-butyl benzoate substituents at the imide termini of the PDI units. Since the chirality is locked, these bis-PDI macrocycles are configurationally stable due to the high free energy barrier (Figure 18b). The configurational stability provides excellent evidence for the "intramolecular somersault" mechanism, which could be confirmed by the single crystal structure (Figure 18c). Moreover, CPL-Laser scanning confocal microscopy was first used to quantify the degree of emitted light circular polarization, and CPL is amplified in the single crystals with a dissymmetry factor value up to 6×10^{-2}. Remarkably, the racemic crystals exhibit both intramolecular H-type $\pi-\pi$ stacking and intermolecular J-type $\pi-\pi$ stacking (Figure 18d), which extend the $\pi-\pi$ self-assembly and impart the assemblies with unique chiroptical and charge/energy transport properties.

3. Summary and Outlook

This review summarizes recent advancements in chiral macrocycles based on central, axial, helical, and planar chiral elements. Each chiral type imparts unique structural and chiroptical properties, enabling applications in enantioselective

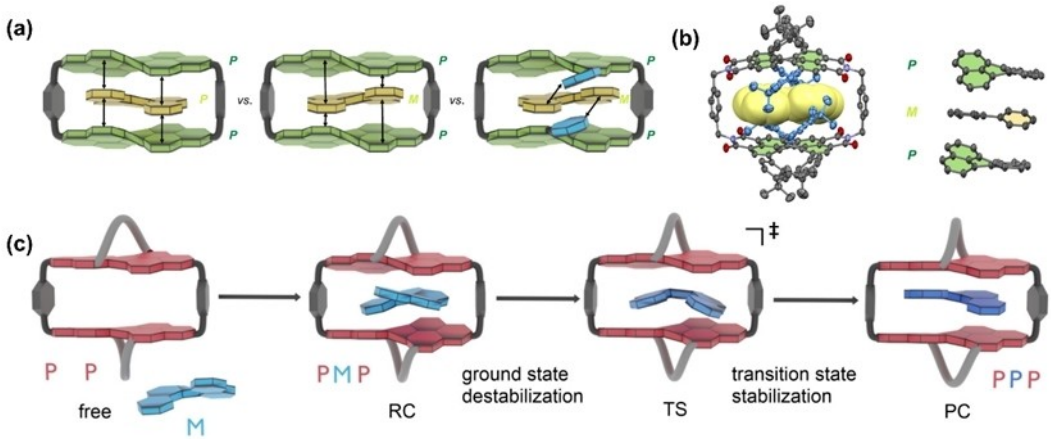

Figure 17. (a) Encapsulation of heterochiral guests by PBI cyclophanes; (b) Single crystal X-ray analysis of a heterochiral complex; (c) The enantiomerization process of [5]helicene within **1-*PP***.

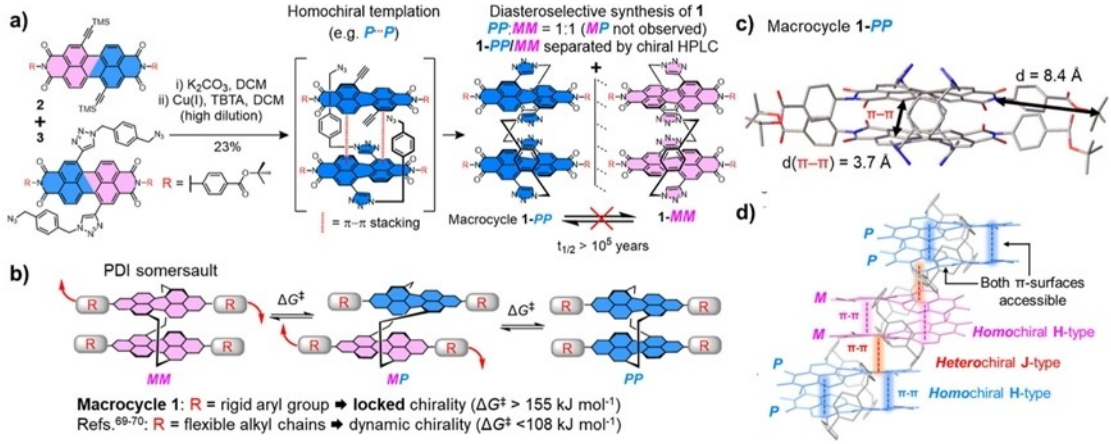

Figure 18. (a) The diastereoselective synthesis of macrocycle **1**; (b) A cartoon of the "intramolecular somersault" mechanism for the interconversion of bis-PDI macrocycle stereoisomers; (c) X-ray crystal structure of macrocycle **1-*PP***; (d) Packing of **1**-rac in the X-ray crystal structure.

recognition, asymmetric catalysis, and CPL. π-conjugated chiral macrocycles with rigid, twisted cavities—primarily those with helical and axial chirality—show promise for chiral optoelectronic applications like CPL due to their unique nanostructures and intrinsic electronic properties.

Planar chiral macrocycles, especially in macrocyclic arenes, have garnered recent interest due to the stereodynamic nature of planar chirality, with various tuning methods yielding novel insights. Central chirality is simpler to introduce, and combining it with other chiral types, particularly planar chirality, enhances self-assembly properties.

Achieving a balance between rigidity and flexibility is essential for effective molecular design. While rigid receptors enhance chiral recognition, flexibility supports exchange, regulation, and cooperativity, which is crucial for asymmetric catalysis and adaptable receptor-substrate interactions. Flexibility also impacts self-assembly processes, potentially leading to new discoveries. CPL research in chiral macrocycles has expanded from single molecules to chiral aggregates, highlighting the importance of combining static and dynamic design features—a complex but valuable pursuit. Asymmetric catalysis applications are still in early stages, and the area of supramolecular macrocycle assemblies remains both promising and evolving, likely driving ongoing research in the field. We hope this review encourages further advancements in chiral macrocycle research.

Acknowledgements

We are grateful for the financial support from the National Key Research & Development Program of China (2016YFA0602900), the National Natural Science Foundation of China (22071066, 22071065), the Natural Science Foundation of Guangdong Province (2024A1515011664).

Conflict of Interests

The authors declare no conflict of interest.

Data Availability Statement

The data that support the findings of this study are available from the corresponding author upon reasonable request.

Keywords: Chiral macrocycles · Enantioselective recognition · Circularly polarized luminescence · Asymmetric catalysis

[1] J. R. Brandt, F. Salerno, M. J. Fuchter, *Nat. Rev. Chem.* **2017**, *1*, 0045.
[2] L. J. Chen, H. B. Yang, M. Shionoya, *Chem. Soc. Rev.* **2017**, *46*, 2555–2576.
[3] G. Albano, G. Pescitelli, L. Di Bari, *Chem. Rev.* **2020**, *120*, 10145–10243.
[4] C. Du, Z. Li, X. Zhu, G. Ouyang, M. Liu, *Nat. Nanotechnol.* **2022**, *17*, 1294–1302.
[5] G. Long, R. Sabatini, M. I. Saidaminov, G. Lakhwani, A. Rasmita, X. Liu, E. H. Sargent, W. Gao, *Nat. Rev. Mater.* **2020**, *5*, 423–439.
[6] E. M. G. Jamieson, F. Modicom, S. M. Goldup, *Chem. Soc. Rev.* **2018**, *47*, 5266–5311.
[7] Y. Zhang, S. Yu, B. Han, Y. Zhou, X. Zhang, X. Gao, Z. Tang, *Matter* **2022**, *5*, 837–875.
[8] T. Zhang, Y. Zhang, Z. He, T. Yang, X. Hu, T. Zhu, Y. Zhang, Y. Tang, J. Jiao, *Chem. - Asian J.* **2024**, *19*, e202400049 .
[9] L. Pasteur, *Compt. Rend.* **1848**, *26*, 535–538.
[10] M. A. Mateos-Timoneda, M. Crego-Calama, D. N. Reinhoudt, *Chem. Soc. Rev.* **2004**, *33*, 363–372.
[11] Y. Wang, J. Xu, Y. Wang, H. Chen, *Chem. Soc. Rev.* **2013**, *42*, 2930–2962.
[12] X. Han, C. Yuan, B. Hou, L. Liu, H. Li, Y. Liu, Y. Cui, *Chem. Soc. Rev.* **2020**, *49*, 6248–6272.
[13] Y. Wu, M. Li, Z. G. Zheng, Z. Q. Yu, W. H. Zhu, *J. Am. Chem. Soc.* **2023**, *145*, 12951–12966.
[14] J. H. Li, X. K. Li, J. Feng, W. Yao, H. Zhang, C. J. Lu, R. R. Liu, *Angew. Chem. Int. Ed.* **2024**, *63*, e202319289.
[15] P. Peluso, B. Chankvetadze, *Chem. Rev.* **2022**, *122*, 13235–13400.
[16] J.-M. Lehn, *Angew. Chem. Int. Ed.* **1988**, *27*, 89–112.
[17] J. L. Atwood, G. W. Gokel, L. J. Barbour, *Comprehensive Supramolecular Chemistry II*, Elsevier, Boston, **2017**.
[18] C. Gagnon, É. Godin, C. Minozzi, J. Sosoe, C. Pochet, S. K. Collins, *Science* **2020**, *367*, 917.
[19] R. López, C. Palomo, *Angew. Chem. Int. Ed.* **2022**, *61*, e202113504.

[20] Y. Liu, Q. Zhang, S. Crespi, S. Chen, X. K. Zhang, T. Y. Xu, C. S. Ma, S. W. Zhou, Z. T. Shi, H. Tian, B. L. Feringa, D. H. Qu, *Angew. Chem. Int. Ed.* **2021**, *60*, 16129–16138.
[21] P. Dominique, M. Schnurr, B. Lewandowski, *Chem. Commun.* **2021**, *57*, 3476–3479.
[22] J. Guo, J. Hou, J. Hu, Y. Geng, M. Li, H. Wang, J. Wang, Q. Luo, *Chem. Commun.* **2023**, *59*, 9157–9166.
[23] R. Aav, E. Shmatova, I. Reile, M. Borissova, F. Topic, K. Rissanen, *Org. Lett.* **2013**, *15*, 3786–3789.
[24] S. Wiegmann, G. Fukuhara, B. Neumann, H. G. Stammler, Y. Inoue, J. Mattay, *Eur. J. Org. Chem.* **2013**, *2013*, 1240–1245.
[25] K. Wada, M. Suzuki, T. Kakuta, T. Yamagishi, S. Ohtani, S. Fa, K. Kato, S. Akine, T. Ogoshi, *Angew. Chem. Int. Ed.* **2023**, *62*, e202217971.
[26] K. Kato, S. Ohtani, M. Gon, K. Tanaka, T. Ogoshi, *Chem Sci* **2022**, *13*, 13147–13152.
[27] J. F. Chen, J. D. Ding, T. B. Wei, *Chem. Commun.* **2021**, *57*, 9029–9039.
[28] X. X. Zhang, J. S. Bradshaw, R. M. Izatt, *Chem. Rev.* **1997**, *97*, 3313–3362.
[29] C. Wang, L. Xu, Z. Jia, T.-P. Loh, *Chin. Chem. Lett.* **2024**, *35*, 109075.
[30] A. Szumna, *Chem. Soc. Rev.* **2010**, *39*, 4274–4285.
[31] Y. Ohishi, M. Murase, H. Abe, M. Inouye, *Org. Lett.* **2019**, *21*, 6202–6207.
[32] J. J. Zhao, K. Zeng, T. X. Jin, W. T. Dou, H. B. Yang, L. Xu, *Coord. Chem. Rev.* **2024**, *502*, 215598.
[33] L. P. Yang, X. Wang, H. Yao, W. Jiang, *Acc. Chem. Res.* **2020**, *53*, 198–208.
[34] L. Xu, H. Liu, X. Peng, P. Shen, B. Z. Tang, Z. Zhao, *Angew. Chem. Int. Ed.* **2023**, *62*, e202300492.
[35] Y. Yang, N. Li, J. Miao, X. Cao, A. Ying, K. Pan, X. Lv, F. Ni, Z. Huang, S. Gong, C. Yang, *Angew. Chem. Int. Ed.* **2022**, *61*, e202202227.
[36] Z. Chen, C. Zhong, J. Han, J. Miao, Y. Qi, Y. Zou, G. Xie, S. Gong, C. Yang, *Adv. Mater.* **2022**, *34*, e2109147.
[37] M. Li, Y. F. Wang, D. Zhang, L. Duan, C. F. Chen, *Angew. Chem. Int. Ed.* **2020**, *59*, 3500–3504.
[38] S. Lin, Y. Tang, W. Kang, H. K. Bisoyi, J. Guo, Q. Li, *Nat. Commun.* **2023**, *14*, 3005.
[39] M. Zhang, Q. Guo, Z. Li, Y. Zhou, S. Zhao, Z. Tong, Y. Wang, G. Li, S. Jin, M. Zhu, T. Zhuang, S. H. Yu, *Sci. Adv.* **2023**, *9*, eadi9944.
[40] M. Hasegawa, Y. Nojima, Y. Mazaki, *ChemPhotoChem* **2021**, *5*, 1042–1058.
[41] Y. Xue, Y. Shi, P. Chen, *Adv. Opt. Mater.* **2024**, *12*, 2303322.
[42] W. Shang, X. Zhu, Y. Jiang, J. Cui, K. Liu, T. Li, M. Liu, *Angew. Chem. Int. Ed.* **2022**, *61*, e202210604.
[43] M. Kwit, J. Grajewski, P. Skowronek, M. Zgorzelak, J. Gawronski, *Chem. Rec.* **2019**, *19*, 213–237.
[44] Y. Wang, H. Wu, J. F. Stoddart, *Acc. Chem. Res.* **2021**, *54*, 2027–2039.
[45] Y. Wang, H. Wu, L. O. Jones, M. A. Mosquera, C. L. Stern, G. C. Schatz, J. F. Stoddart, *J. Am. Chem. Soc.* **2023**, *145*, 1855–1865.
[46] D. J. Kim, K. R. Hermann, A. Prokofjevs, M. T. Otley, C. Pezzato, M. Owczarek, J. F. Stoddart, *J. Am. Chem. Soc.* **2017**, *139*, 6635–6643.
[47] Y. Wu, S. K. Nalluri, R. M. Young, M. D. Krzyaniak, E. A. Margulies, J. F. Stoddart, M. R. Wasielewski, *Angew. Chem. Int. Ed.* **2015**, *54*, 11971–11977.
[48] L. Pu, *Acc. Chem. Res.* **2012**, *45*, 150–163.
[49] Y. Yu, Y. Hu, C. Ning, W. Shi, A. Yang, Y. Zhao, Z. Cao, Y. Xu, P. Du, *Angew. Chem. Int. Ed.* **2024**, *63*, e202407034.
[50] Y. Nojima, M. Hasegawa, N. Hara, Y. Imai, Y. Mazaki, *Chem. Commun.* **2019**, *55*, 2749–2752.
[51] M. Hasegawa, C. Hasegawa, Y. Nagaya, K. Tsubaki, Y. Mazaki, *Chem. - Eur. J.* **2022**, *28*, e202202218.
[52] K. Miki, T. Noda, M. Gon, K. Tanaka, Y. Chujo, Y. Mizuhata, N. Tokitoh, K. Ohe, *Chem. - Eur. J.* **2019**, *25*, 9211–9216.
[53] R. Fu, Q. Y. Zhao, H. Han, W. L. Li, F. Y. Chen, C. Tang, W. Zhang, S. D. Guo, D. Y. Li, W. C. Geng, D. S. Guo, K. Cai, *Angew. Chem. Int. Ed.* **2023**, *62*, e202315990.
[54] R. Fu, D. Y. Li, J. H. Tian, Y. L. Lin, Q. Y. Zhao, W. L. Li, F. Y. Chen, D. S. Guo, K. Cai, *Angew. Chem. Int. Ed.* **2024**, *63*, e202406233.
[55] H. Han, R. Fu, R. Wang, C. Tang, M. M. He, J. Y. Deng, D. S. Guo, J. F. Stoddart, K. Cai, *J. Am. Chem. Soc.* **2022**, *144*, 20351–20362.
[56] G. Sun, X. Zhang, Z. Zheng, Z.-Y. Zhang, M. Dong, J. L. Sessler, C. Li, *J. Am. Chem. Soc.* **2024**, *146*, 26233–26242.
[57] R. Ning, H. Zhou, S. X. Nie, Y. F. Ao, D. X. Wang, Q. Q. Wang, *Angew. Chem. Int. Ed.* **2020**, *59*, 10894–10898.
[58] K. Yamashita, Y. Tabata, K. Yamakawa, T. Mochizuki, K. Matsui, M. Hatano, K. Ishihara, *J. Am. Chem. Soc.* **2023**, *145*, 26238–26248.
[59] L. W. Zhang, X. D. Wang, Y. F. Ao, D. X. Wang, Q. Q. Wang, *Chem. - Eur. J.* **2024**, *30*, e202400498.
[60] K. Takaishi, S. Murakami, F. Yoshinami, T. Ema, *Angew. Chem. Int. Ed.* **2022**, *61*, e202204609.
[61] K. Takaishi, F. Yoshinami, Y. Sato, T. Ema, *Chem. - Eur. J.* **2024**, *30*, e202400866.
[62] Y. Wang, Q. Liao, Y. Feng, Q. Meng, *J. Mol. Struct.* **2024**, *1304*, 137695.
[63] M. Hu, H.-T. Feng, Y.-X. Yuan, Y.-S. Zheng, B. Z. Tang, *Coord. Chem. Rev.* **2020**, *416*, 213329.
[64] M. Hu, F. Y. Ye, C. Du, W. Wang, W. Yu, M. Liu, Y. S. Zheng, *Angew. Chem. Int. Ed.* **2022**, *61*, e202115216.
[65] Y.-X. Yuan, M. Hu, K.-R. Zhang, T.-T. Zhou, S. Wang, M. Liu, Y.-S. Zheng, *Mater. Horiz.* **2020**, *7*, 3209–3216.
[66] A. Garci, S. Abid, A. H. G. David, M. D. Codesal, L. Đorđević, R. M. Young, H. Sai, L. Le Bras, A. Perrier, M. Ovalle, P. J. Brown, C. L. Stern, A. G. Campaña, S. I. Stupp, M. R. Wasielewski, V. Blanco, J. F. Stoddart, *Angew. Chem. Int. Ed.* **2022**, *61*, e202208679.
[67] X. Jiang, J. D. Laffoon, D. Chen, S. Perez-Estrada, A. S. Danis, J. Rodriguez-Lopez, M. A. Garcia-Garibay, J. Zhu, J. S. Moore, *J. Am. Chem. Soc.* **2020**, *142*, 6493–6498.
[68] F. Aribot, A. Merle, P. Dechambenoit, H. Bock, A. Artigas, N. Vanthuyne, Y. Carissan, D. Hagebaum-Reignier, Y. Coquerel, F. Durola, *Angew. Chem. Int. Ed.* **2023**, *62*, e202304058.
[69] W. Fan, T. Matsuno, Y. Han, X. Wang, Q. Zhou, H. Isobe, J. Wu, *J. Am. Chem. Soc.* **2021**, *143*, 15924–15929.
[70] J. Malincik, S. Gaikwad, J. P. Mora-Fuentes, M. A. Boillat, A. Prescimone, D. Haussinger, A. G. Campana, T. Solomek, *Angew. Chem. Int. Ed.* **2022**, *61*, e202208591.
[71] F. Zhao, J. Zhao, H. Liu, Y. Wang, J. Duan, C. Li, J. Di, N. Zhang, X. Zheng, P. Chen, *J. Am. Chem. Soc.* **2023**, *145*, 10092–10103.
[72] G. Sabapathi, A. Prasad Nambiar, P. Nag, R. Mariam Ipe, S. Reddy Vennapusa, *Angew. Chem. Int. Ed.* **2023**, *62*, e202306566.
[73] R. S. Cahn, C. K. Ingold, V. J. E. Prelog, *Experientia* **1956**, *12*, 81–94.
[74] Y. Fan, J. He, L. Liu, G. Liu, S. Guo, Z. Lian, X. Li, W. Guo, X. Chen, Y. Wang, H. Jiang, *Angew. Chem. Int. Ed.* **2023**, *62*, e202304623.
[75] C. D. Gutsche, *Acc. Chem. Res.* **1982**, *16*, 161–170.
[76] V. Böhmer, *Angew. Chem. Int. Ed.* **1995**, *34*, 713–745.
[77] N. Morohashi, F. Narumi, N. Iki, T. Hattori, S. Miyano, *Chem. Rev.* **2006**, *106*, 5291–5316.
[78] Y. K. Agrawal, J. P. Pancholi, J. M. Vyas, *J. Sci. Ind. Res.* **2008**, *68*, 745–768.
[79] S. Tong, J. T. Li, D. D. Liang, Y. E. Zhang, Q. Y. Feng, X. Zhang, J. Zhu, M. X. Wang, *J. Am. Chem. Soc.* **2020**, *142*, 14432–14436.
[80] J. H. Chen, Z. Y. Jiang, H. Xiao, S. Tong, T. H. Shi, J. Zhu, M. X. Wang, *Angew. Chem. Int. Ed.* **2023**, *62*, e202301782.
[81] Y. Z. Zhang, M. M. Xu, X. G. Si, J. L. Hou, Q. Cai, *J. Am. Chem. Soc.* **2022**, *144*, 22858–22864.
[82] T. Ogoshi, S. Kanai, S. Fujinami, T. A. Yamagishi, Y. Nakamoto, *J. Am. Chem. Soc.* **2008**, *130*, 5022–5023.
[83] T. Ogoshi, T. A. Yamagishi, Y. Nakamoto, *Chem. Rev.* **2016**, *116*, 7937–8002.
[84] K. Kato, S. Fa, T. Ogoshi, *Angew. Chem. Int. Ed.* **2023**, *62*, e202308316.
[85] S. Fa, T. Kakuta, T. A. Yamagishi, T. Ogoshi, *Chem. Lett.* **2019**, *48*, 1278–1287.
[86] X. Hu, Y. Tian, P. Chen, *Tetrahedron* **2024**, *162*.
[87] K. Kato, R. Iwano, S. Tokuda, K. Yasuzawa, M. Gon, S. Ohtani, S. Furukawa, K. Tanaka, T. Ogoshi, *Aggregate* **2024**, *5*, e482.
[88] H. Zhu, Q. Li, Z. Gao, H. Wang, B. Shi, Y. Wu, L. Shangguan, X. Hong, F. Wang, F. Huang, *Angew. Chem. Int. Ed.* **2020**, *59*, 10868–10872.
[89] S. Fa, M. Mizobata, S. Nagano, K. Suetsugu, T. Kakuta, T. A. Yamagishi, T. Ogoshi, *ACS Nano* **2021**, *15*, 16794–16801.
[90] J. F. Chen, X. Yin, B. Wang, K. Zhang, G. Meng, S. Zhang, Y. Shi, N. Wang, S. Wang, P. Chen, *Angew. Chem. Int. Ed.* **2020**, *59*, 11267–11272.
[91] J. Li, H. Y. Zhou, Y. Han, C. F. Chen, *Angew. Chem. Int. Ed.* **2021**, *60*, 21927–21933.
[92] Y. F. Wang, H. Yao, L. P. Yang, M. Quan, W. Jiang, *Angew. Chem. Int. Ed.* **2022**, *61*, e202211853.
[93] H. Zhou, X. Y. Pang, X. Wang, H. Yao, L. P. Yang, W. Jiang, *Angew. Chem. Int. Ed.* **2021**, *60*, 25981–25987.
[94] X. Yang, W. Jiang, *J. Am. Chem. Soc.* **2024**, *146*, 3900–3909.
[95] X. Tian, M. Zuo, Y. Shen, N. Mao, K. Wang, Y. Sheng, K. Velmurugan, J. Jiao, X. Y. Hu, *Nat. Commun.* **2024**, *15*, 7182.
[96] K. Velmurugan, A. Murtaza, A. Saeed, J. Li, K. Wang, M. Zuo, Q. Liu, X.-Y. Hu, *CCS Chem.* **2022**, *4*, 3426–3439.
[97] C. Tu, W. Wu, W. Liang, D. Zhang, W. Xu, S. Wan, W. Lu, C. Yang, *Angew. Chem. Int. Ed.* **2022**, *61*, e202203541.

[98] Y. Guo, Y. Han, X.-S. Du, C.-F. Chen, *ACS Appl. Polym. Mater.* **2022**, *4*, 3473–3481.
[99] H. Nian, L. Cheng, L. Wang, H. Zhang, P. Wang, Y. Li, L. Cao, *Angew. Chem. Int. Ed.* **2021**, *60*, 15354–15358.
[100] S. Guo, L. Liu, X. Li, G. Liu, Y. Fan, J. He, Z. Lian, H. Yang, X. Chen, H. Jiang, *Small* **2024**, *20*, e2308429.
[101] J. Wang, G. Zhuang, M. Chen, D. Lu, Z. Li, Q. Huang, H. Jia, S. Cui, X. Shao, S. Yang, P. Du, *Angew. Chem. Int. Ed.* **2020**, *59*, 1619–1626.
[102] Q. Shi, X. Wang, B. Liu, P. Qiao, J. Li, L. Wang, *Chem. Commun.* **2021**, *57*, 12379–12405.
[103] J. Wang, H. Shi, S. Wang, X. Zhang, P. Fang, Y. Zhou, G. L. Zhuang, X. Shao, P. Du, *Chem. - Eur. J.* **2022**, *28*, e202103828.
[104] B. Jiang, Y. Han, S. Wu, Z. Li, J. Wu, *ACS Appl. Nano Mater.* **2022**, *5*, 14027–14030.
[105] X. N. Han, P. F. Li, Y. Han, C. F. Chen, *Angew. Chem. Int. Ed.* **2022**, *61*, e202202527.
[106] M. Lin, L. Bian, Q. Chen, H. Xu, Z. Liu, K. Zhu, *Angew. Chem. Int. Ed.* **2023**, *62*, e202303035.
[107] M. Hecht, P. Leowanawat, T. Gerlach, V. Stepanenko, M. Stolte, M. Lehmann, F. Wurthner, *Angew. Chem. Int. Ed.* **2020**, *59*, 17084–17090.
[108] F. Li, Y. Li, G. Wei, Y. Wang, S. Li, Y. Cheng, *Chem. - Eur. J.* **2016**, *22*, 12910–12915.
[109] L. Zhang, I. Song, J. Ahn, M. Han, M. Linares, M. Surin, H. J. Zhang, J. H. Oh, J. Lin, *Nat. Commun.* **2021**, *12*, 142.
[110] Y. Liu, Z. Ma, Z. Wang, W. Jiang, *J. Am. Chem. Soc.* **2022**, *144*, 11397–11404.
[111] P. Osswald, F. J. J. O. T. A. C. S. Würthner, *J. Am. Chem. Soc.* **2007**, *129*, 14319–14326.
[112] J. Li, P. Li, M. Fan, X. Zheng, J. Guan, M. Yin, *Angew. Chem. Int. Ed.* **2022**, *61*, e202202532.
[113] M. Weh, K. Shoyama, F. Würthner, *Nat. Commun.* **2023**, *14*, 243.
[114] P. Spenst, F. Wurthner, *Angew. Chem. Int. Ed.* **2015**, *54*, 10165–10168.
[115] G. Ouyang, J. Ruhe, Y. Zhang, M. J. Lin, M. Liu, F. Wurthner, *Angew. Chem. Int. Ed.* **2022**, *61*, e202206706.
[116] M. Weh, A. A. Kroeger, K. Shoyama, M. Grune, A. Karton, F. Wurthner, *Angew. Chem. Int. Ed.* **2023**, *62*, e202301301.
[117] S. E. Penty, M. A. Zwijnenburg, G. R. F. Orton, P. Stachelek, R. Pal, Y. Xie, S. L. Griffin, T. A. Barendt, *J. Am. Chem. Soc.* **2022**, *144*, 12290–12298.
[118] S. E. Penty, G. R. F. Orton, D. J. Black, R. Pal, M. A. Zwijnenburg, T. A. Barendt, *J. Am. Chem. Soc.* **2024**, *146*, 5470–5479.

Manuscript received: November 15, 2024
Accepted manuscript online: December 14, 2024
Version of record online: January 8, 2025